GSK-3 is a master regulator of neural progenitor homeostasis

Woo-Yang Kim[1], **Xinshuo Wang**[1], **Yaohong Wu**[1], **Bradley W Doble**[2], **Satish Patel**[3], **James R Woodgett**[3], and **William D Snider**[1]

[1]Neuroscience Center, University of North Carolina School of Medicine, Chapel Hill, North Carolina, USA

[2]McMaster Stem Cell and Cancer Research Institute, McMaster University, Hamilton, Ontario, Canada

[3]Samuel Lunenfeld Research Institute, Mount Sinai Hospital and Department of Medical Biophysics, University of Toronto, Toronto, Ontario, Canada

Abstract

The development of the brain requires the exquisite coordination of progenitor proliferation and differentiation to achieve complex circuit assembly. It has been suggested that glycogen synthase kinase 3 (GSK-3) acts as an integrating molecule for multiple proliferation and differentiation signals because of its essential role in the RTK, Wnt and Shh signaling pathways. We created conditional mutations that deleted both the α and β forms of GSK-3 in mouse neural progenitors. GSK-3 deletion resulted in massive hyperproliferation of neural progenitors along the entire neuraxis. Generation of both intermediate neural progenitors and postmitotic neurons was markedly suppressed. These effects were associated with the dysregulation of β-catenin, Sonic Hedgehog, Notch and fibroblast growth factor signaling. Our results indicate that GSK-3 signaling is an essential mediator of homeostatic controls that regulate neural progenitors during mammalian brain development.

GSK-3 is a serine-threonine kinase with established roles in receptor tyrosine kinase and Wnt/Frizzled signaling. In mammals, the GSK-3 family consists of two members, GSK-3α and GSK-3β, which have 98% sequence identity in their kinase domains. Recent studies that have mostly used pharmacological approaches have suggested that GSK-3 is important in an array of settings including regulation of transcription factor levels in multiple signaling pathways, cell polarity and neurotransmitter signaling[1–3]. Recently, pharmacological evidence has implicated GSK-3 signaling in the regulation of embryonic stem cell self-renewal[4–6]. Furthermore, it has been suggested that the Deleted in Schizophrenia (DISC1), which has been implicated in some familial cases of schizophrenia and depression, regulates

neural progenitor proliferation and may act in part via regulation of GSK-3 activity[7]. These observations raise the question of how GSK-3 functions in relation to neural progenitor self-renewal and neurogenesis during brain development.

Development of the brain requires exquisite coordination of progenitor proliferation and differentiation to achieve optimized functional potential. Recently, multiple signaling pathways, including Wnts, fibroblast growth factors (FGFs), Sonic Hedgehog (Shh) and Notch, have been identified as regulating neural progenitors[8]. However, the manner in which these signals are coordinated to achieve exquisite spatial and temporal control over neurogenesis is unknown. GSK-3s are uniquely well-positioned to coordinate multiple proliferation and differentiation signals because they potentially regulate critical nodes in each of these pathways. Inhibition of GSK-3 is critical to canonical Wnt signaling leading to increased β-catenin levels in all of the cell types studied to date[1]. Furthermore, GSK-3 is inhibited downstream of FGF signaling via phosphatidylinositol-3 kinase (PI3K)[9]. Several recent studies in cell lines have demonstrated GSK-3 regulation of Myc family proteins via the PI3K pathway[10–13]. In *Drosophila*, it is known that the GSK-3 homolog Shaggy regulates Hedgehog signaling[14]. Finally, several studies in cell lines have demonstrated that GSK-3 inhibition modulates the Notch pathway[15–17]. To date, however, the effects of deleting GSK-3 specifically in neural progenitors on signaling via these pathways and on progenitor self-renewal and subsequent brain development have not been determined.

We used a conditional knockout strategy in a *Gsk3a* null background to specifically target *Gsk3b* in the developing nervous system. We found that GSK-3–deficient progenitors were locked into the radial progenitor phase, as generation of both intermediate neural progenitors (INPs) and postmitotic neurons was markedly suppressed. Our findings suggest that GSK-3 deletion removes homeostatic controls on neural progenitors, shifting the balance toward self-renewal and away from neurogenesis.

RESULTS

GSK-3 deletion markedly enhances progenitor proliferation

To investigate the functions of GSK-3 in the developing mammalian nervous system, we generated *Gsk3a*$^{-/-}$ (*Gsk3a* null) and *Gsk3b*$^{loxP/loxP}$ mice and crossed these with a well-characterized *nestin-cre* line that drives expression of Cre recombinase in CNS progenitors from about embryonic day 10 (E10)[18,19]. *Gsk3a* null mice that harbored an exon 2 deletion and *Gsk3b*$^{loxP/loxP}$ mice were generated by flanking exon 2 with *loxP* sites (Supplementary Fig. 1)[20,21]. Neither *Gsk3a* null nor *Gsk3b*$^{loxP/loxP}$; *nestin-cre* mice had major brain developmental malformations (W.-Y.K. and W.D.S., unpublished observations)[22]. Western blots showed that the α and β forms of GSK-3 were eliminated in the developing brains of *Gsk3a*$^{-/-}$; *GSK Gsk3b*$^{loxP/loxP}$; *nestin-cre* mice (Supplementary Fig. 1). Compared with the control littermates (*Gsk3a*$^{+/-}$; *Gsk3b*$^{loxP/+}$; *nestin-cre*), *Gsk3a*$^{-/-}$; *Gsk3b*$^{loxP/loxP}$; *nestin-cre* mice had bigger heads (Supplementary Fig. 1) at every developmental stage from E12.5 until they died at P0. Brains from control mice had smooth and straight cortices in coronal sections at E13.5 (Supplementary Fig. 1), whereas the brains of *Gsk3a*$^{-/-}$ *Gsk3b*$^{loxP/loxP}$; *nestin-cre* mice were markedly convoluted. *Gsk3a*$^{-/-}$ *Gsk3b*$^{loxP/loxP}$; *nestin-cre* brains also showed substantially enlarged ventral brain areas, including the ganglionic eminence and

ventral thalamus (Supplementary Fig. 1). We measured the ventricular apical surface lengths and found a 2.7-fold increase in GSK-3–deleted brains compared with control brains (Supplementary Fig. 1).

To explore the basis of the convoluted cortex, we assessed neural progenitors in the $Gsk3a^{-/-}$; $Gsk3b^{loxP/loxP}$; nestin-cre brain using an antibody to Sox2, a neural progenitor marker. In control brains at E13.5, Sox2-positive progenitors were distinctly distributed surrounding the ventricles (Fig. 1a). We also observed Sox2 expression in a limited part of the dorsal ganglionic eminence. In $Gsk3a^{-/-}$; $Gsk3b^{loxP/loxP}$; nestin-cre brains, Sox2-positive neural progenitor pools were massively expanded (Fig. 1a). At the level of ganglionic eminence, this expansion was also prominent in ventral forebrain. We observed this progenitor expansion at every rostro-caudal level that we examined, including spinal cord (Fig. 1a).

To further assess this hyperproliferation, we measured the proportion of cells in various cell-cycle phases at E13.5. Twice as many cells were positive per coronal section for the mitotic marker phosphohistone H3 in $Gsk3a^{-/-}$; $Gsk3b^{loxP/loxP}$; nestin-cre cerebral cortex compared with controls (Fig. 1b,c and Supplementary Fig. 2). Western blotting confirmed that phospho-histone H3 expression was markedly increased (Supplementary Fig. 2). We then assessed the numbers cells in S phase after a short-term BrdU pulse. The number of BrdU-positive S phase cells was also increased (Fig. 1b,c and Supplementary Fig. 2). These results indicate that many more cells were undergoing division in $Gsk3a^{-/-}$; $Gsk3b^{loxP/loxP}$; nestin-cre brains than in controls at E13.5. To further identify the underlying causes of the expansion of the progenitor pool, we investigated cell-cycle length and re-entry. The number of Ki67 and BrdU double-positive cells after short and long BrdU pulses in $Gsk3a^{-/-}$; $Gsk3b^{loxP/loxP}$; nestin-cre cortex was increased (Fig. 1c), indicating both a shortening of the cell cycle and increased cell-cycle re-entry. Immunostaining and western blotting with an antibody to activated caspase-3 revealed that levels of apoptosis were not significantly different between control and mutant cortex at E13.5 ($P < 0.01$; Fig. 1c and Supplementary Fig. 2). Taken together, these results indicate that the expanded progenitor pool in $Gsk3a^{-/-}$; $Gsk3b^{loxP/loxP}$; nestin-cre brain is the result of increases in cell-cycle rate and re-entry, but not of enhanced progenitor survival.

GSK-3 deletion strongly Inhibits neurogenesis

To assess the progression of the radial progenitors to INPs, we immunostained cerebral cortex samples using an antibody to Tbr2, a specific marker for INPs[23]. To our surprise, we found that the number of Tbr2-positive cells was reduced by 64% (±2.7%) in $Gsk3a^{-/-}$; $Gsk3b^{loxP/loxP}$; nestin-cre cortices (Fig. 2a). Western blotting showed that the level of Tbr2 in $Gsk3a^{-/-}$; $Gsk3b^{loxP/loxP}$; nestin-cre brain was markedly decreased (Fig. 2b). Our results indicate that GSK-3 activity is required to regulate the conversion of Sox2-positive radial progenitors into INPs during cortical development.

We next examined the number of neurons in both control and mutant sections using immunostaining with an antibody to Tuj1 that recognizes postmitotic neurons. The numbers of Tuj1–positive neurons were decreased by about 60% in $Gsk3a^{-/-}$; $Gsk3b^{loxP/loxP}$; nestin-cre cortical sections (Fig. 3). We observed similar decreases with Tbr1 and NeuN, two commonly used neuronal markers (Fig. 3b–d). These morphological results were confirmed

by western blotting. The levels of the neuronal makers Tuj1, MAP2, SMI32 and NeuN in *Gsk3a*$^{-/-}$*; Gsk3b*$^{loxP/loxP}$*; nestin-cre* brain tissue were all reduced by 50–70% (Fig. 3e,f). In contrast, the progenitor markers Nestin and Pax6 were upregulated by 100–200%. Together, these results indicate that GSK-3 is required for proper regulation of neuro-genesis in the developing mouse brain.

To assess the effects on neurogenesis over time, we examined *Gsk3a*$^{-/-}$*; Gsk3b*$^{loxP/loxP}$*; nestin-cre* brains at multiple rostro-caudal levels at E15.5 (Fig. 4). Notably, we observed that there was massive expansion of the area filled with Sox2-positive cells throughout the telencephalon in *Gsk3a*$^{-/-}$*; Gsk3b*$^{loxP/loxP}$*; nestin-cre* cortical wall in comparison with controls, where Sox2-positive progenitors were restricted to regions surrounding the ventricles (Fig. 4a–d). Neurogenesis in GSK-3 mutant brains at this age was strongly suppressed, as marked by Tuj1 staining (Fig. 4e,f). Thus, inhibition of neurogenesis is persistent in the absence of GSK-3 signaling.

One implication of our findings is that GSK-3 activity toward substrates that influence proliferation may be upregulated as the progenitor proliferation diminishes and as neurogenesis proceeds. To assess this idea in a general way, we measured the phosphorylation levels of c-Myc and β-catenin, GSK-3 targets, at three developmental stages, E13, E15 and E17. Both phospho–c-Myc and phospho–β-catenin levels in brain lysates were increased with increasing embryonic age (Supplementary Fig. 3), suggesting that GSK-3 activity toward the proliferation regulators c-Myc and β-catenin is suppressed during the period of active progenitor proliferation and increased at later stages.

Activation of β-catenin, Shh and Notch signaling

To determine whether Wnt signaling is involved in the expansion of the progenitor pool in *Gsk3a*$^{-/-}$*; Gsk3b*$^{loxP/loxP}$*; nestin-cre* brains, we first examined the expression levels and the distribution patterns of β-catenin. In controls, β-catenin was highly enriched along the apical surface (Fig. 5a). However, in *Gsk3a*$^{-/-}$*; Gsk3b*$^{loxP/loxP}$*; nestin-cre* brains, β-catenin was highly expressed throughout the thickness of the developing cortex (Fig. 5a). We also observed a similar loss of the normal spatial expression pattern and an increase in the levels of β-catenin in the spinal cord (Supplementary Fig. 4). At the single-cell level, we found an increased level of β-catenin in both the nucleus and the cytosol in GSK-3 mutant brains (Fig. 5a), indicating accumulation and translocation of β-catenin from the cytosolic compartment to the nucleus. Western blots showed that total levels of β-catenin and its transcriptional targets Axin2 and c-Jun were increased in *Gsk3a*$^{-/-}$*; Gsk3b*$^{loxP/loxP}$*; nestin-cre* brains (Fig. 5b). Together, these data indicate that β-catenin is markedly dysregulated in *Gsk3a*$^{-/-}$*; Gsk3b*$^{loxP/loxP}$*; nestin-cre* neural progenitors and suggest that β-catenin/TCF/LEF1 signaling is hyperactive in these cells.

To further investigate the mechanisms responsible for the expanded progenitor pool, we examined Shh signaling. We first examined overall levels of Shh downstream effectors, Gli1 and Gli2 proteins in *Gsk3a*$^{-/-}$*; Gsk3b*$^{loxP/loxP}$*; nestin-cre* brains at E14.5. Western blots showed that levels of Gli1 and Gli2 were markedly increased, whereas levels of Gli3 were unchanged (Fig. 5). Gli1 has been demonstrated to be a direct transcriptional target of Gli2 in neural and non-neural systems[24]. Therefore, we determined the distribution patterns of

Gli1 mRNAs in *Gsk3a*$^{-/-}$*; Gsk3b*$^{loxP/loxP}$*; nestin-cre* brains using *in situ* hybridization. *Gli1* was strongly expressed in the ventricular/subventricular zone of GSK-3 mutant dorsal telencephalon, whereas there was little expression in control dorsal telencephalon (Fig. 5d). Furthermore, we found a massive expansion of *Gli1* expression in mutant ventral telencephalon (Fig. 5d). *Patched*, a transcriptional target of Shh signaling[24], was also markedly upregulated, particularly in dorsal regions of the ganglionic eminence (Fig. 5d). The increased levels of Shh components were not associated with Shh protein levels, as no changes were found in Shh expression between control and GSK-3–deleted brain samples (Supplementary Fig. 5). To test whether the increases in the levels of Shh components are functionally relevant, we knocked downed *Gli1* in dissociated *Gsk3a*$^{-/-}$*; Gsk3b*$^{loxP/loxP}$*; nestin-cre* progenitors using small interfering RNA to *Gli1*. The siRNA decreased the progenitor proliferation by about 35% compared with controls (Supplementary Fig. 5). These data indicate that Shh signaling is constitutively activated in *Gsk3a*$^{-/-}$*; Gsk3b*$^{loxP/loxP}$*; nestin-cre* brains and that Shh signaling is important in mediating GSK-3 deletion effects.

Finally, to determine whether there may be abnormal activation of Notch signaling in *Gsk3a*$^{-/-}$*; Gsk3b*$^{loxP/loxP}$*; nestin-cre* brains, we examined the expression level and distribution pattern of Hes1, a Notch downstream mediator. Hes1 expression is normally restricted to the ventricular and subventricular zones (Fig. 6a). However, we found that Hes1 was distributed throughout the width of the cerebral cortical wall of GSK-3 mutants. The overall levels of Hes1 and Hes5 were also substantially increased in *Gsk3a*$^{-/-}$*; Gsk3b*$^{loxP/loxP}$*; nestin-cre* brain lysates (Fig. 6b). The widespread distribution and upregulation of Hes1 suggests that the Notch pathway is activated in the developing cortex of *Gsk3a*$^{-/-}$*; Gsk3b*$^{loxP/loxP}$*; nestin-cre* embryos. To address this possibility, we measured the amount of cleaved intracellular domain of Notch (NICD, activated form of Notch) that was present. We found that, compared with control brains, the amount of NICD in *Gsk3a*$^{-/-}$*; Gsk3b*$^{loxP/loxP}$*; nestin-cre* brains was markedly increased (Fig. 6c). To assess the increase in Notch signaling is functionally relevant, we treated GSK-3–deleted progenitors with the gamma secretase inhibitor *N*-[*N*-(3,5-difluorophenacetyl-L-alanyl)]-S- phenylglycine *t*-butyl ester (DAPT). This treatment reduced the hyperproliferation and increased the number of MAP2-positive neurons (Supplementary Fig. 6). We conclude that inactivation of endogenous GSK-3 enhances Notch signaling, which then inhibits neurogenesis in *Gsk3a*$^{-/-}$*; Gsk3b*$^{loxP/loxP}$*; nestin-cre* mice.

Both constitutive and targeted activation of β-catenin enhances the proliferation of neural progenitors[25,26]. These findings raise the questions of whether the effects of GSK-3 deletion that we observed are entirely mediated by increased levels of β-catenin. To address this issue, we inhibited β-catenin signaling by transfecting dissociated *Gsk3a*$^{-/-}$*; Gsk3b*$^{loxP/loxP}$*; nestin-cre* cortical progenitors with a dominant- negative TCF (*dnTCF*) construct that lacks the N-terminal sequences required for β-catenin binding[27]. Overexpression of *dnTCF* only partially inhibited proliferation of GSK-3–deleted progenitors, reducing proliferation markers by about 50% (Fig. 6d,e). The percentage of proliferating cells was still almost twice as high as that of controls (Supplementary Fig. 6). Thus, a substantial fraction of GSK-3–deleted progenitors continued to proliferate when β-catenin signaling was suppressed. Notably, inhibition of Notch signaling by transfection of a dominant-negative Hes1 (*dnHes1*) also resulted in reductions of progenitor proliferation by around 50% (Fig.

6d,e). However, inhibition of both β-catenin and Notch signaling reduced proliferation in GSK-3–deleted cells to levels below 5% (Fig. 6d,e). These results are consistent with the idea that independent regulation of β-catenin and Notch signaling mediate GSK-3's effects.

GSK-3 regulation of c-Myc downstream of FGF/PI3K

Myc family proteins are critical for the regulation of proliferation in multiple settings and GSK-3 has been shown to directly regulate the stability of both c-Myc and the related family member N-Myc in cell lines[10]. We stained *Gsk3a*^{−/−}*; Gsk3b*[loxP/loxP]*; nestin-cre* progenitors with an antibody to c-Myc and found that there was a massive accumulation of c-Myc proteins in the nucleus (Fig. 7a). Western blots confirmed the major increase of c-Myc and N-Myc in *Gsk3a*^{−/−}*; Gsk3b*[loxP/loxP]*; nestin-cre* brain samples that we observed (Fig. 7b). GSK-3 phosphorylation of c-Myc (and N-Myc) at T58 is thought to promote c-Myc degradation through ubiquitin-proteasome machinery. We found that T58 phosphorylation was almost completely abrogated in GSK-3 mutant brain samples, as predicted (Fig. 7b). To test whether the increase in c-Myc levels is functionally relevant, we inhibited c-Myc function in dissociated *Gsk3a*^{−/−}*; Gsk3b*[loxP/loxP]*; nestin-cre* progenitors with a dominant–negative c-Myc (dnc-Myc) construct in a procedure similar to the one outlined above for β-catenin. Overexpression of dnc-Myc decreased progenitor proliferation by 41 ± 5% compared with a green fluorescent protein (GFP) overexpression control.

GSK-3 regulation of Myc protein stability is thought to occur downstream of PI3K signaling. A logical candidate to regulate this signaling would be the FGFs, which are known to regulate progenitor proliferation in the developing telencephalon via receptor tyrosine kinases[8]. Therefore, we examined the possibility that GSK-3 mediates FGF-PI3K signaling in the regulation of neural progenitor proliferation. We assessed progenitor proliferation in control and GSK-3–deficient cortical cultures after treatment with FGF2 and/or LY294002. As expected, addition of FGF2 increased progenitor proliferation in control cultures (data not shown). Treatment with LY294002 decreased the numbers of BrdU-positive proliferating progenitors in FGF2-treated control cultures by more than 50% (Fig. 7c,d). Notably, the inhibitory effects of LY294002 were completely suppressed in *Gsk3a*^{−/−}*; Gsk3b*[loxP/loxP]*; nestin-cre* cortical cultures.

We next assessed c-Myc levels in cortical cultures while inhibiting PI3K and stimulating FGF. Treatment of control cortical cultures with LY294002 substantially decreased c-Myc levels (Supplementary Fig. 7). As expected, phosphorylation of c-Myc at T58 and GSK-3β at S9 were increased and decreased, respectively. These results suggest that inhibition of PI3K decreases c-Myc levels by enhancing GSK-3 activity. To address this possibility, we performed the same experiments in *Gsk3a*^{−/−}*; Gsk3b*[loxP/loxP]*; nestin-cre* cortical cultures. The decrease in c-Myc levels that we observed with LY294002 treatment was abolished in the lysates of GSK-3β–deleted cultures (Fig. 7e). To assess the potential regulation of c-Myc levels by FGF2, we treated cortical cultures with FGF2. Treatment with FGF2 markedly upregulated c-Myc and this was inhibited by LY294002 (Fig. 7f). The increase of c-Myc in GSK-3–deficient cortical cells was not affected by treatment with either FGF2 or FGF2 and LY294002 (Fig. 7f). Taken together, these results strongly suggest that GSK-3 mediates FGF-PI3K regulation of c-Myc.

Multiple studies have shown that appropriate apical-basal polarity of progenitors is required for normal neurogenesis[28]. To address progenitor polarity, we stained brain tissues with antibodies against multiple cell polarity and adhesion markers including PKCζ, cadherin, actin, APC and EB1. The polarized apical concentrations of the markers were significantly reduced in the cortex of $Gsk3a^{-/-}$; $Gsk3b^{loxP/loxP}$; nestin-cre animals (Supplementary Fig. 8). These results demonstrate that GSK-3 signaling is essential for apical-basal polarity in the developing cortex and suggest that GSK-3 may control progenitor proliferation in part by organizing cellular polarity.

DISCUSSION

GSK-3 is an important molecular regulator of neurogenesis

We found that deletion of GSK-3 massively expanded the radial progenitor pool. The elimination of either GSK-3 family member alone or the elimination of three $Gsk3$ alleles had no obvious effect. This suggests that a major reduction of GSK-3 signaling is required to remove critical GSK-3–mediated homeostatic controls during embryonic brain development.

Determination of the mitotic index with phospho-histone H3, BrdU and Ki67 labeling indicated that premature re-entry and shortening of the cell cycle occurred in progenitors in $Gsk3a^{-/-}$; $Gsk3b^{loxP/loxP}$; nestin-cre mice. Shortened cell cycle has previously been implicated in reduced responsiveness to differentiation signals and it has been suggested that cell-cycle regulation is an important control point for mechanisms that account for differences in neuron number between rodents and primates[29]. In contrast with the expansion of Sox2-positive radial progenitors, generation of neurons and INPs was markedly reduced in the absence of GSK-3. Thus, neural differentiation was arrested at the radial progenitor stage. The effects of GSK-3 deletion on proliferation and differentiation that we observed suggest that temporal and spatial regulation of GSK-3 activity during nervous system development is required to terminate proliferation and allow differentiation at just the right moment to yield the correct number of neurons. Our results raise the possibility that regulation of the activity of a single kinase provides a powerful and simple mechanism for controlling neuron number.

GSK-3 deletion removes multiple homeostatic controls

The extent to which the multiple mechanisms that are known to regulate neural progenitors operate independently or are coordinately regulated is unclear. GSK-3 has the, to the best of our knowledge, unique potential to control each of these critical homeostatic mechanisms.

Dysregulation of β-catenin levels is likely to be important for the hyperproliferation of progenitors that we observed. Our findings are entirely consistent with the notion that appropriate regulation of β-catenin is critical for the control of progenitor proliferation in multiple regions of the developing nervous system[7,25,26,30–32]. Shh signaling is also affected by GSK-3 deletion. Our results suggest that there is a mammalian counterpart of the *Drosophila* GSK-3 homolog Shaggy, which regulates cubitus interruptus (a homolog of mammalian Gli proteins) in the *Drosophila* Hedgehog signaling pathway[14]. The increased proliferation and regulation of Shh signaling components observed in the ventral

telencephalon of GSK-3–deleted mutants strongly suggest that GSK-3 is a critical mediator of Shh signaling in this region. GSK-3 is therefore a candidate for integrating Wnt/β-catenin and Shh signaling pathways, both of which are known to control neurogenesis in the ventral telencephalon[32].

Our data also indicate that Notch signaling is increased in GSK-3–deficient brains. Notch signaling is known to be important for the maintenance of 'stemness' and the identity of radial glial cells during development[33–35]. Notably, Notch signaling levels distinguish radial progenitors from INPs that have attenuated canonical Notch signaling[34]. Our results are consistent with the idea that high levels of Notch signaling in *Gsk3a⁻/⁻; Gsk3b^{loxP/loxP}; nestin-cre* cells suppress neurogenesis at the stage of radial progenitors as they self-renew and that few cells progress to become Tbr2-positive INPs.

Potential interactions among GSK-3–regulated pathways

An important issue is whether GSK-3 regulation leads to a hierarchy of signaling mechanisms that regulate progenitor proliferation or whether multiple GSK-3–regulated mechanisms each contribute independently to the final outcome. There is some evidence that β-catenin can influence Notch signaling and can be regulated by the FGF pathway[9]. However, we doubt that stabilization of β-catenin alone fully accounts for the effects that we describe here and suggest that several other GSK-3–regulated mechanisms exert independent effects. Elimination of β-catenin in neural progenitors reduces, but does not eliminate, progenitor proliferation *in vivo*[30,32]. Our data indicate that overexpression of *dnTCF* only partially inhibits proliferation in *Gsk3a⁻/⁻; Gsk3b^{loxP/loxP}; nestin-cre* neural progenitors *in vitro*. These results suggest that GSK-3 deletion may result in effects on Notch signaling that are independent of β-catenin. Several studies have suggested that GSK-3 may directly regulate Notch signaling via phosphorylation of Notch1 or Notch2, or regulate the actions of the gamma secretase presenillin-1 (refs. 15–17). However, all of this work has been carried out in cell lines and the importance of these findings *in vivo* is unclear.

Finally, our data indicate that GSK-3 strongly regulates Myc family proteins and that FGF regulation of c-Myc via PI3K signaling is disrupted by GSK-3 deletion. Myc family proteins are critical for the regulation of proliferation in multiple settings and a Myc family member, N-Myc, is known from mouse genetic studies to be required for the maintenance of neural progenitor proliferation in cerebellum and cortex[10]. Because c-Myc is thought to be a transcriptional target of β-catenin[36,37], at least some of the observed increase of c-Myc in GSK-3–deleted progenitors may be attributable to β-catenin effects. However, we found another mechanism of c-Myc regulation, in which FGF-PI3K controls c-Myc levels via GSK-3. Our findings are consistent with work in cell lines demonstrating that GSK-3 signaling can directly regulate the stability of Myc family proteins via PI3K signaling[11–13]. Indeed, we found that GSK-3 phosphorylation of c-Myc at T58, which is thought to be important for its stability, is regulated by PI3K. This FGF–PI3K–GSK-3 regulation of Myc protein stability in neural progenitors is likely to be critical for determining its effects, as the half-life of Myc protein in cell lines is extraordinarily brief, on the order of 20 min[38].

ONLINE METHODS

Materials

DAPT (Calbiochem), recombinant human basic FGF2 (Sigma), recombinant human epidermal growth factor (EGF) (R&D system), B27 supplements (Invitrogen), N2 supplement (Invitrogen), BrdU (Sigma) and LY294002 (Cell Signaling) were purchased from the companies indicated. Plasmids encoding wild-type and a constitutively active β-catenin were generously provided by B. Vogelstein (Johns Hopkins University). Dominant-negative TCF, Hes1 and c-Myc were generous gifts from A. Chenn (Northwestern University), A. Strom (Karolinska Institute) and H. Sugimura (Hamamatsu University), respectively. *Gli1* siRNAs were obtained from Invitrogen.

Mice

Mice were cared for according to animal protocols approved by the Institutional Animal Care and Use Committees of the University of North Carolina and University of Toronto. *Gsk3a*$^{-/-}$ mice were engineered to harbor an exon 2 deletion[20]. *Gsk3b*$^{loxP/loxP}$ mice were generated so that exon 2 is flanked by *loxP* sites[21]. Nervous system–specific conditional GSK-3 double-knockout mice (*Gsk3a*$^{-/-}$; *Gsk3b*$^{loxP/loxP}$; *nestin-cre*) were generated by mating *Gsk3a*$^{-/-}$, *Gsk3b*$^{loxP/loxP}$ and *nestin-cre* mice[18]. Littermate *Gsk3a*$^{+/-}$; *Gsk3b*$^{loxP/+}$; *nestin-cre* mice served as controls.

Immunohistochemistry

Immunohistochemical labeling of embryonic brain sections or dissociated neural cells was performed as previously described[22]. For primary antibodies, we used rabbit antibody to Sox2 (Chemicon), mouse antibody to Nestin (BD biosciences), rabbit antibody to Tbr1 (Chemicon), rabbit antibody to Tbr2 (Abcam), rabbit antibody to phospho-histone H3 (Upstate Biotech), mouse antibody to BrdU (Sigma), rabbit antibody to Ki67 (Covance), rabbit antibody to caspase 3 (Cell Signaling), rabbit antibody to β-catenin (Cell Signaling), mouse antibody to Tuj1 (Sigma), mouse antibody to tubulin (Sigma), mouse antibody to NeuN (Chemicon), rabbit antibody to PKCζ (Cell signaling), rabbit antibody to cadherin (Cell Signaling), mouse antibody to actin (Sigma), rabbit antibody to APC (gift from K. Neufeld, University of Kansas), mouse antibody to EB1 (Sigma), mouse antibody to γ-tubulin (Sigma), rabbit antibody to Hes1 (Santa Cruz), rabbit antibody to c-Myc (Cell Signaling) or mouse antibody to GSK-3β (BD Biosciences). Appropriate Cy2-, Cy3- or Alexa dye–conjugated secondary antibodies (Jackson ImmunoResearch, Molecular Probes) were used to detect primary antibody binding. DAPI (Sigma) or Draq5 (Molecular probes) was used as nuclear counterstains.

Morphometry

For the quantification of brain size and ventricular apical surface length, we imaged ten different cresyl violet–stained brain sections at periodic distances along the rostro-caudal axis. The area of each section was defined using the Freehand selection tool in ImageJ (US National Institutes of Health). The calculated ImageJ values were averaged and the result was recalculated as relative changes versus control. The same brain sections were used to

measure ventricular apical surface lengths of control and *Gsk3a*$^{-/-}$*; Gsk3b*$^{loxP/loxP}$*; nestin-cre* brains. Ventricular apical surface length was defined using the Freehand line selection tool in ImageJ.

For cell counts, images were taken with a Zeiss LSM510 confocal microscope and a Nikon Eclipse epifluorescence microscope. For image analysis, the Zeiss LSM510 image browser and Metamorph software (Molecular Devices) were used. The numbers of neural progenitors and neurons positive for BrdU, phospho-histone H3, Ki67, Sox2, MAP2, Tuj1, Tbr1 or NeuN were obtained as previously described[25,39].

BrdU administration and quantification of mitosis

For proliferation assays, intraperitoneal injection was performed into pregnant mice at E11–14. BrdU (20 mg per kg of body weight, dissolved in 0.9% saline, wt/vol) was administered either 24 h or 30 min before the mouse was killed for transient assays.

The mitotic index is a ratio of the number of phospho-histone H3–positive cells to the number of DAPI-stained cells per field. To analyze the BrdU labeling index and cell-cycle re-entry, we exposed E13 control and *Gsk3a*$^{-/-}$*; Gsk3b*$^{loxP/loxP}$*; nestin-cre* mice to BrdU. Then brain slices were immunostained with antibodies to BrdU and Ki67. The BrdU labeling index is the fraction of progenitor cells (Ki67 and BrdU double positive) to the number of BrdU-positive cells after a 30-min BrdU pulse label. For the analysis of cell-cycle re-entry, mice were exposed to a single-pulse BrdU label for 24 h. The fraction of cells labeled with BrdU and Ki67 relative to the total number of BrdU-positive cells after a 24-h pulse label was determined.

Western blotting

Extracts from E13.5 telencephalon was prepared using RIPA buffer and the protein content was determined by a Bio-Rad Protein Assay system. Proteins were separated on 3–8% or 4–12% SDS-PAGE gradient gels and transferred onto nitrocellulose membrane. The membrane was incubated with mouse antibody to GSK-3 (Invitrogen), rabbit antibody to phospho–GSK-3β (Cell signaling), mouse antibody to actin (Sigma), rabbit antibody to phospho-histone H3 (Upstate), rabbit antibody to activated caspase 3 (Cell Signaling), rabbit antibody to Tbr2 (Abcam), mouse antibody to Tuj1 (Sigma), mouse antibody to MAP2 (Chemicon), mouse antibody to NeuN (Chemicon), mouse antibody to Pax6 (Iowa Hybridoma Bank), mouse antibody to Nestin (BD Biosciences), rabbit antibody to β-catenin (Cell Signaling), SMI32 (Sternberger Immunocytochemicals), rabbit antibody to c-Myc (Cell Signaling), mouse antibody to N-Myc (Santa Cruz), rabbit antibody to c-Jun (Cell Signaling), rabbit antibody to Hes1 (Santa Cruz), rabbit antibody to NICD (Cell Signaling), rabbit antibody to Gli1 (Cell Signaling), rabbit antibody to Gli2 (Abcam), rabbit antibody to Gli3 (Santa Cruz), rabbit antibody to phospho-AKT (Cell Signaling), rabbit antibody to phospho-MEK (Cell Signaling), rabbit antibody to phospho-ERK (Cell Signaling), rabbit antibody to GluR (Cell Signaling) or rabbit antibody to GAPDH (Cell Signaling) at 4 °C overnight. As secondary antibodies, we used donkey antibody to mouse or rabbit IgG conjugated to horseradish peroxidase (Amersham). ECL reagents (Amersham) were used for immunodetection.

For quantification of band intensity, blots from three independent experiments for each molecule of interest were used. Signals were measured using ImageJ software and represented by relative intensity versus that of control. GAPDH was used as an internal control to normalize band intensity.

Progenitor cultures

Cerebral cortex from E11–14 mice dorsal telencephalon was isolated and dissociated with trituration after trypsin/EDTA treatment. Then, the cells were plated onto poly-D-lysine/laminin–coated coverslips and cultured for 2 d in the medium containing neurobasal medium, B27 and N2 supplements, FGF2 (10 ng ml^{-1}), and EGF (10 ng ml^{-1}). For differentiation of neural progenitors, the medium containing FGF2 and EGF was removed and replaced by neurobasal medium with 5% serum (vol/vol), B27 and N2 supplements. To assess the numbers of proliferating progenitors and differentiated neurons, we carried out immunostaining and morphometry using antibodies to Ki67, phospho-histone H3 and MAP2, as described above. More than 20 random microscopic fields (10× and 20×) were analyzed for each condition.

For capturing images of the cultures, we used Metamorph software and a Hamamatsu Orca ER CCD camera attached to a Nikon Eclipse microscope. All image analysis for the measurement of proliferating cells was done with IPLab software (Scanalytics) or Metamorph software.

Electroporation

Mouse cortical progenitors were transfected with various plasmids as described previously[22]. First, embryonic cortices were dissociated and suspended in 100 μl of Amaxa electroporation buffer with 2–10 μg of plasmid DNA. Then, suspended cells were transferred to an Amaxa electroporation cuvette and electroporated with an Amaxa Nucleofector apparatus set on the G-13 program. After electroporation, cells were plated onto coated coverslips and the medium was changed 4 h later to remove the remnant transfection buffer.

dnTCF and dnc-Myc lack the β-catenin–binding domain and transactivation domain, respectively. dnHes1 has a mutated DNA-binding domain. A ratio of the number of Ki67 and GFP double-positive cells to the number of GFP-positive transfected cells was determined using the sampling methods outlined above.

In situ hybridization

For riboprobe synthesis, we used the pBSII plasmids containing *Gli1* and *Patched* (A. Joyner, Memorial Sloan-Kettering Cancer Institute). A 1,600-bp E*coR*I fragment containing a zinc-finger domain was used to generate antisense *Gli1* riboprobe. Patched riboprobe was synthesized from an 841-bp *EcoR*I fragment. Digoxigenin-labeled riboprobes were synthesized using *in vitro* transcription. Paraformaldehyde-fixed (4%, wt/vol) frozen brains from E12–14 embryos were sectioned at 20 μm, treated with proteinase K (0.5 μg ml^{-1}), acetylated, dehydrated according to standard protocols and hybridized with digoxigenin-labeled riboprobes (1 μg ml^{-1}) for 18 h at 65 °C. Then, the tissue sections were rinsed and incubated with a 1:2,000 dilution of alkaline phosphatase–conjugated sheep antibody to

digoxigenin (Roche) in blocking buffer for 3 h at 20–25 °C and developed using nitro-blue tetrazolium chloride and 5-bromo-4-chloro-3′-indolyphosphate p-toluidine salt according to the manufacturer's instructions. After developing, alkaline phosphatase activity was quenched by fixation in 4% paraformaldehyde and slides containing tissue sections were mounted in Aquatex (EM Science Harleco).

Statistical analysis

For examining tissue sections, we used six E12–16 mice for each experiment (control mice, $n = 3$; $Gsk3a^{-/-}$; $Gsk3b^{loxP/loxP}$; nestin-cre mice, $n = 3$). Random fields chosen from more than ten tissue sections from each embryo were examined. For assessing cultured progenitors and neurons, more than 20 random fields from three mice were analyzed for each condition. Statistical significance was determined using an independent t test and one-way ANOVA followed by Tukey's post hoc test. Data are presented as means ± s.e.m.

Supplementary Material

Refer to Web version on PubMed Central for supplementary material.

Acknowledgments

References

1. Doble BW, Woodgett JR. GSK-3: tricks of the trade for a multi-tasking kinase. J Cell Sci. 2003; 116:1175–1186. [PubMed: 12615961]

2. Kockeritz L, Doble B, Patel S, Woodgett JR. Glycogen synthase kinase-3: an overview of an over-achieving protein kinase. Curr Drug Targets. 2006; 7:1377–1388. [PubMed: 17100578]

3. Beaulieu JM, Gainetdinov RR, Caron MG. The Akt–GSK-3 signaling cascade in the actions of dopamine. Trends Pharmacol Sci. 2007; 28:166–172. [PubMed: 17349698]

4. Sato N, Meijer L, Skaltsounis L, Greengard P, Brivanlou AH. Maintenance of pluripotency in human and mouse embryonic stem cells through activation of Wnt signaling by a pharmacological GSK-3-specific inhibitor. Nat Med. 2004; 10:55–63. [PubMed: 14702635]

5. Ying QL, et al. The ground state of embryonic stem cell self-renewal. Nature. 2008; 453:519–523. [PubMed: 18497825]

6. Bone HK, et al. Involvement of GSK-3 in regulation of murine embryonic stem cell self-renewal revealed by a series of bisindolylmaleimides. Chem Biol. 2009; 16:15–27. [PubMed: 19171302]

7. Mao Y, et al. Disrupted in schizophrenia 1 regulates neuronal progenitor proliferation via modulation of GSK3beta/beta-catenin signaling. Cell. 2009; 136:1017–1031. [PubMed: 19303846]

8. Corbin JG, et al. Regulation of neural progenitor cell development in the nervous system. J Neurochem. 2008; 106:2272–2287. [PubMed: 18819190]

9. Shimizu T, et al. Stabilized beta-catenin functions through TCF/LEF proteins and the Notch/RBP-Jkappa complex to promote proliferation and suppress differentiation of neural precursor cells. Mol Cell Biol. 2008; 28:7427–7441. [PubMed: 18852283]

10. Knoepfler PS, Kenney AM. Neural precursor cycling at sonic speed: N-Myc pedals, GSK-3 brakes. Cell Cycle. 2006; 5:47–52. [PubMed: 16322694]

11. Bechard M, Dalton S. Subcellular localization of glycogen synthase kinase 3beta controls embryonic stem cell self-renewal. Mol Cell Biol. 2009; 29:2092–2104. [PubMed: 19223464]

12. Doble BW, Woodgett JR. Exploring pluripotency with chemical genetics. Cell Stem Cell. 2009; 4:98–100. [PubMed: 19200796]

13. Otto T, et al. Stabilization of N-Myc is a critical function of Aurora A in human neuroblastoma. Cancer Cell. 2009; 15:67–78. [PubMed: 19111882]

14. Jia J, et al. Shaggy/GSK3 antagonizes Hedgehog signaling by regulating Cubitus interruptus. Nature. 2002; 416:548–552. [PubMed: 11912487]

15. Espinosa L, Ingles-Esteve J, Aguilera C, Bigas A. Phosphorylation by glycogen synthase kinase 3 beta downregulates Notch activity, a link for Notch and Wnt pathways. J Biol Chem. 2003; 278:32227–32235. [PubMed: 12794074]

16. Uemura K, et al. GSK3beta activity modifies the localization and function of presenilin 1. J Biol Chem. 2007; 282:15823–15832. [PubMed: 17389597]

17. Jin YH, Kim H, Oh M, Ki H, Kim K. Regulation of Notch1/NICD and Hes1 expressions by GSK-3alpha/beta. Mol Cells. 2009; 27:15–19. [PubMed: 19214430]

18. Tronche F, et al. Disruption of the glucocorticoid receptor gene in the nervous system results in reduced anxiety. Nat Genet. 1999; 23:99–103. [PubMed: 10471508]

19. Yokota Y, et al. The adenomatous polyposis coli protein is an essential regulator of radial glial polarity and construction of the cerebral cortex. Neuron. 2009; 61:42–56. [PubMed: 19146812]

20. MacAulay K, et al. Glycogen synthase kinase 3alpha–specific regulation of murine hepatic glycogen metabolism. Cell Metab. 2007; 6:329–337. [PubMed: 17908561]

21. Patel S, et al. Tissue-specific role of glycogen synthase kinase 3beta in glucose homeostasis and insulin action. Mol Cell Biol. 2008; 28:6314–6328. [PubMed: 18694957]

22. Kim WY, et al. Essential roles for GSK-3s and GSK-3–primed substrates in neurotrophin-induced and hippocampal axon growth. Neuron. 2006; 52:981–996. [PubMed: 17178402]

23. Sessa A, Mao CA, Hadjantonakis AK, Klein WH, Broccoli V. Tbr2 directs conversion of radial glia into basal precursors and guides neuronal amplification by indirect neurogenesis in the developing neocortex. Neuron. 2008; 60:56–69. [PubMed: 18940588]

24. Ding Q, et al. Diminished Sonic hedgehog signaling and lack of floor plate differentiation in Gli2 mutant mice. Development. 1998; 125:2533–2543. [PubMed: 9636069]

25. Chenn A, Walsh CA. Regulation of cerebral cortical size by control of cell cycle exit in neural precursors. Science. 2002; 297:365–369. [PubMed: 12130776]

26. Woodhead GJ, Mutch CA, Olson EC, Chenn A. Cell-autonomous beta-catenin signaling regulates cortical precursor proliferation. J Neurosci. 2006; 26:12620–12630. [PubMed: 17135424]

27. Chen S, et al. Wnt-1 signaling inhibits apoptosis by activating beta-catenin/T cell factor–mediated transcription. J Cell Biol. 2001; 152:87–96. [PubMed: 11149923]

28. Götz M, Huttner WB. The cell biology of neurogenesis. Nat Rev Mol Cell Biol. 2005; 6:777–788. [PubMed: 16314867]

29. Dehay C, Kennedy H. Cell-cycle control and cortical development. Nat Rev Neurosci. 2007; 8:438–450. [PubMed: 17514197]

30. Zechner D, et al. Beta-catenin signals regulate cell growth and the balance between progenitor cell expansion and differentiation in the nervous system. Dev Biol. 2003; 258:406–418. [PubMed: 12798297]

31. Machon O, et al. A dynamic gradient of Wnt signaling controls initiation of neurogenesis in the mammalian cortex and cellular specification in the hippocampus. Dev Biol. 2007; 311:223–237. [PubMed: 17916349]

32. Gulacsi AA, Anderson SA. Beta-catenin–mediated Wnt signaling regulates neurogenesis in the ventral telencephalon. Nat Neurosci. 2008; 11:1383–1391. [PubMed: 18997789]

33. Yoon K, Gaiano N. Notch signaling in the mammalian central nervous system: insights from mouse mutants. Nat Neurosci. 2005; 8:709–715. [PubMed: 15917835]

34. Mizutani K, Yoon K, Dang L, Tokunaga A, Gaiano N. Differential Notch signaling distinguishes neural stem cells from intermediate progenitors. Nature. 2007; 449:351–355. [PubMed: 17721509]

35. Shimojo H, Ohtsuka T, Kageyama R. Oscillations in notch signaling regulate maintenance of neural progenitors. Neuron. 2008; 58:52–64. [PubMed: 18400163]

36. He TC, et al. Identification of c-MYC as a target of the APC pathway. Science. 1998; 281:1509–1512. [PubMed: 9727977]

37. Calvisi DF, Ladu S, Factor VM, Thorgeirsson SS. Activation of beta-catenin provides proliferative and invasive advantages in c-myc/TGF-alpha hepatocarcinogenesis promoted by phenobarbital. Carcinogenesis. 2004; 25:901–908. [PubMed: 14742323]

38. Eilers M, Eisenman RN. Myc's broad reach. Genes Dev. 2008; 22:2755–2766. [PubMed: 18923074]

39. Cappello S, et al. The Rho-GTPase cdc42 regulates neural progenitor fate at the apical surface. Nat Neurosci. 2006; 9:1099–1107. [PubMed: 16892058]
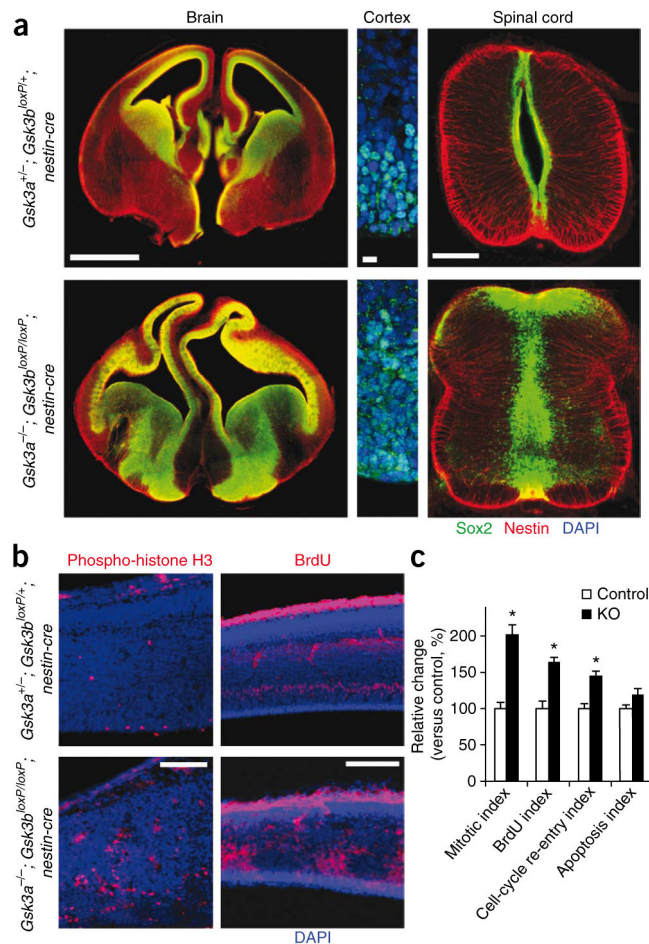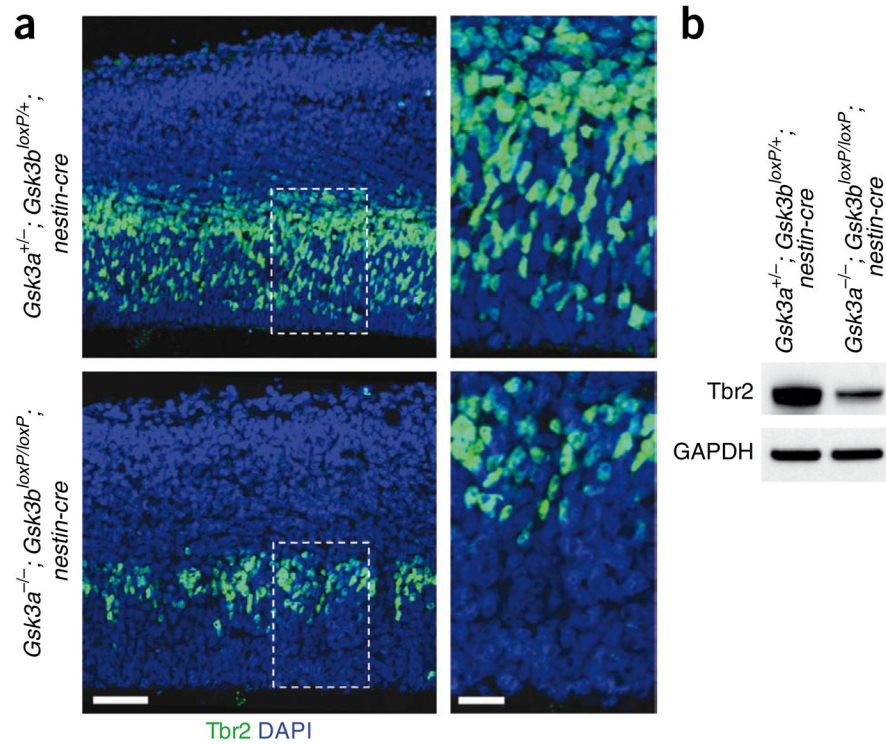
Figure 1.
GSK-3 deletion leads to a massive increase in neural progenitor proliferation. (**a**) Neural progenitor pools are massively expanded in $Gsk3a^{-/-}$; $Gsk3b^{loxP/loxP}$; nestin-cre (KO) mice. Sections of developing forebrain and spinal cord at E13.5 were immunostained with an antibody to Sox2. Left, neural progenitor pools were heavily expanded throughout the cerebral cortex and ventral area in the $Gsk3a^{-/-}$; $Gsk3b^{loxP/loxP}$; nestin-cre brain sections. Scale bar represents 900 μm. Middle, high-magnification image of cerebral cortex immunostained for Sox2. Scale bar represents 10 μm. Right, the central canal was closed as a result of progenitor hyperproliferation in $Gsk3a^{-/-}$; $Gsk3b^{loxP/loxP}$; nestin-cre spinal cord and there was extension of progenitors into the developing dorsal horn. Scale bar represents 200 μm. (**b**) Enhanced progenitor division in $Gsk3a^{-/-}$; $Gsk3b^{loxP/loxP}$; nestin-cre brains. The numbers of phospho-histone H3– and BrdU-positive dividing cells were increased in the sections of $Gsk3a^{-/-}$; $Gsk3b^{loxP/loxP}$; nestin-cre cerebral cortex at E13.5 compared with controls. The phospho-histone H3–labeled mitotic cells were mostly near ventricles in control sections. They were not limited in ventricular region, but rather spread throughout the developing cortical wall in $Gsk3a^{-/-}$; $Gsk3b^{loxP/loxP}$; nestin-cre sections. Scale bars represent 50 μm (left panels) and 100 μm (right panels). (**c**) Quantification of mitotic, BrdU labeling, cell cycle re-entry and apoptosis indices. $n = 10$ sections from each of three mutants and control embryos per each condition. * $P < 0.01$.

Figure 2.
Conversion of radial progenitors to INPs is suppressed by GSK-3 deletion. (**a**) The number of Tbr2-positive INPs was markedly reduced in the *Gsk3a$^{-/-}$; Gsk3b$^{loxP/loxP}$; nestin-cre* brain sections. E13.5 cerebral cortex samples from controls and *Gsk3a$^{-/-}$; Gsk3b$^{loxP/loxP}$; nestin-cre* mice were immunostained with an antibody to Tbr2. Nuclei were counterstained with DAPI. Right panels show higher magnification of small boxes (white dotted) in left panels. Scale bars represent 50 μm (left panels) and 20 μm (right panels). (**b**) Western blotting showed that the level of Tbr2 was markedly reduced in the *Gsk3a$^{-/-}$; Gsk3b$^{loxP/loxP}$; nestin-cre* brain tissues.
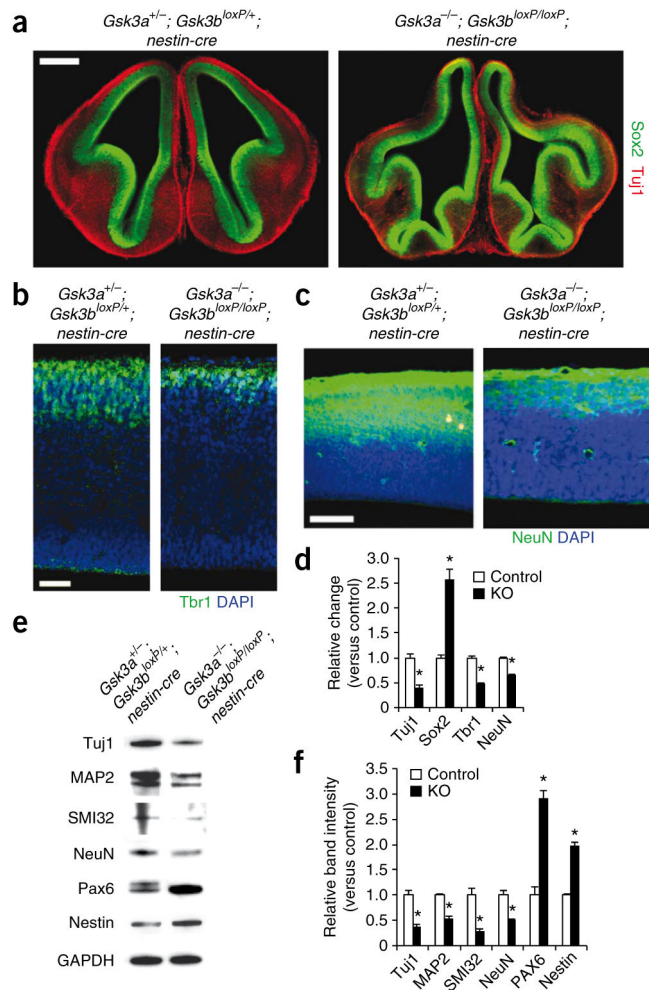
Figure 3.

GSK-3 deletion in progenitors strongly inhibits neurogenesis. (**a**) Marked thinning of cortical areas filled with Tuj1-positive cells in $Gsk3a^{-/-}$; $Gsk3b^{loxP/loxP}$; nestin-cre brain sections at E13.5. Scale bar represents 500 μm. (**b**) This was also observed with Tbr1, a deeper- layer neuron marker, staining. Scale bar represents 50 μm. (**c**) NeuN-positive neurons were also markedly less frequent in $Gsk3a^{-/-}$; $Gsk3b^{loxP/loxP}$; nestin-cre cortical sections. Scale bar represents 100 μm. (**d**) Quantification of Tuj1-, Sox2-, Tbr1- and NeuN-positive cells. The ratios of Tuj1-, Sox2- and Tbr1-positive cells to the DAPI-stained cells per field were measured and shown as relative change versus control. Relative changes of NeuN-positive areas in $Gsk3a^{-/-}$; $Gsk3b^{loxP/loxP}$; nestin-cre tissue samples were scored by measuring NeuN-positive areas with ImageJ software. $n = 10$ sections from each of three mutant and control embryos per each condition. * $P < 0.01$. (**e**) Western blotting showed that the neuronal makers Tuj1, MAP2, SMI32 and NeuN were downregulated in $Gsk3a^{-/-}$; $Gsk3b^{loxP/loxP}$; nestin-cre brain tissues. However, the progenitor markers Nestin and Pax6 were upregulated. Tissue lysates from three mutant and control brains per each condition were used. (**f**) Quantification of western blot data. We used three independent blots from each condition for quantification.
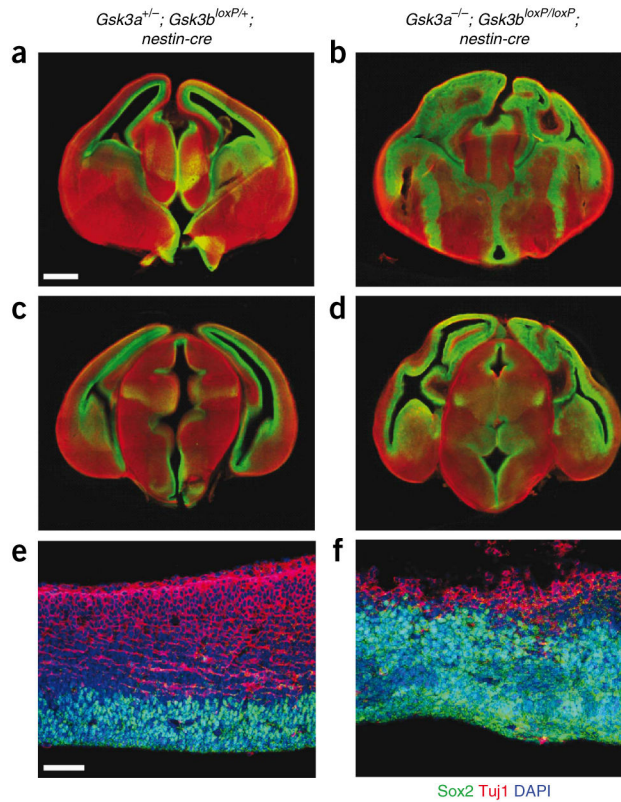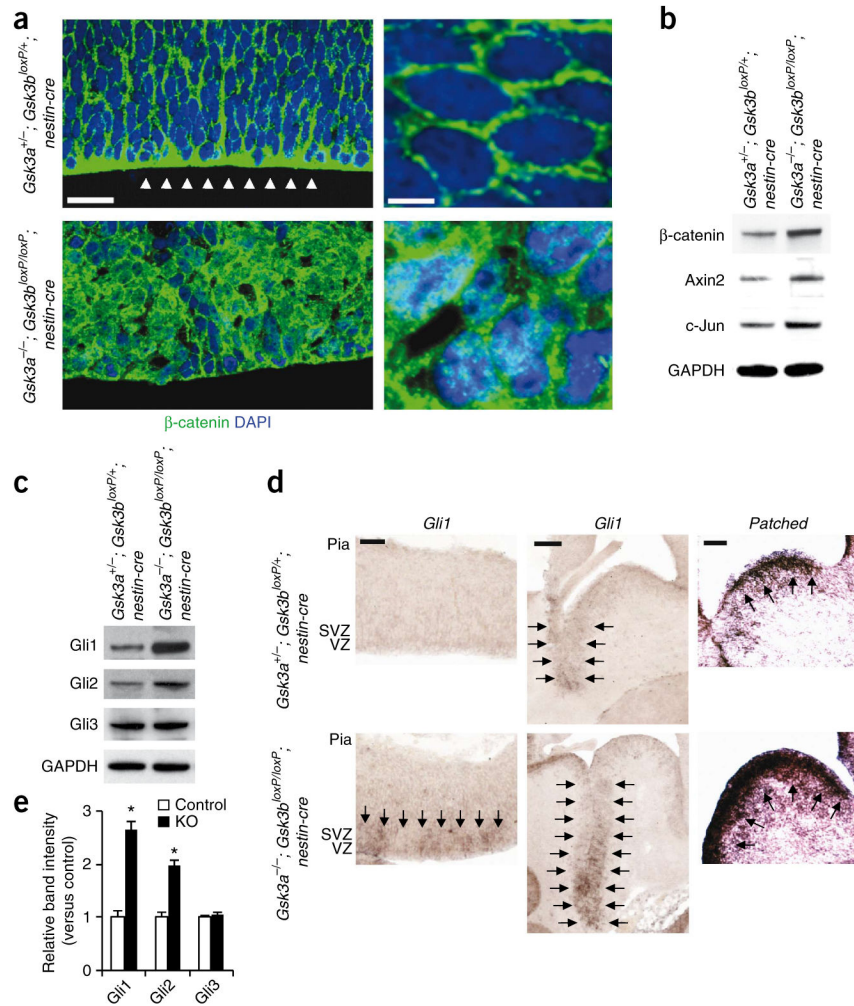
Figure 4.
Neurogenesis is inhibited through E15.5. (**a–d**) The neural progenitor pool was massively expanded throughout the rostro-caudal neuraxis in *Gsk3a$^{-/-}$; Gsk3b$^{loxP/loxP}$; nestin-cre* mice. Serial brain sections in the rostro-caudal direction were prepared from E15.5 mice and were immunostained for Sox2 (green) and Tuj1 (red). Scale bar represents 400 μm. Rostral brain sections are shown in **a** and **b**, and caudal brain sections are shown in **c** and **d**. (**e,f**) Higher magnification showed that Sox2-positive progenitor pools in GSK-3 mutant cortex were even more expanded at E15.5 than at earlier ages. Generation of Tuj1-positive neurons was severely inhibited through this stage. Scale bar represents 100 μm. Left, control brain sections. Right, *Gsk3a$^{-/-}$; Gsk3b$^{loxP/loxP}$; nestin-cre* sections.

Figure 5.
Dysregulation of β-catenin and Shh signaling components as a result of GSK-3 deletion. (**a**) Spatial expression of β-catenin was disrupted in *Gsk3a*$^{-/-}$*; Gsk3b*$^{loxP/loxP}$*; nestin-cre* brain sections. Left, expression of β-catenin was highly enriched along the apical surface of control cortical sections (arrow heads). In mutants, β-catenin was highly expressed throughout the developing cerebral cortical wall. Right, higher-magnification images showing that β-catenin in *Gsk3a*$^{-/-}$*; Gsk3b*$^{loxP/loxP}$*; nestin-cre* sections was present in both the nucleus and cytosol. Scale bars represent 20 μm (left) and 5 μm (right). (**b**) Western blots showed that the expression of β-catenin and its target genes, including *Axin2* and *c-Jun*, were increased in the *Gsk3a*$^{-/-}$*; Gsk3b*$^{loxP/loxP}$*; nestin-cre* brains. (**c**) There were marked increases in Gli1 and Gli2 protein levels in the *Gsk3a*$^{-/-}$*; Gsk3b*$^{loxP/loxP}$*; nestin-cre* brains. (**d**) Shh signaling was enhanced in E14 *Gsk3a*$^{-/-}$*; Gsk3b*$^{loxP/loxP}$*; nestin-cre* brain sections. Left, *Gli1* mRNAs were expressed at low levels in E14 dorsal telencephalon controls. There was a significant induction of *Gli1* in the ventricular and subventricular regions of *Gsk3a*$^{-/-}$*; Gsk3b*$^{loxP/loxP}$*; nestin-cre* samples (arrows). Scale bar represents 100 μm. Middle, there was a marked induction of *Gli1* mRNA levels in *Gsk3a*$^{-/-}$*; Gsk3b*$^{loxP/loxP}$*; nestin-cre* ventral telencephalon (arrows). Scale bar represents 200 μm. Right, *Patched* mRNA in control

tissues was expressed in the dorsal part of the ventral telencephalon. Ventral telencephalic expression of *Patched* mRNAs in *Gsk3a*$^{-/-}$*; Gsk3b*$^{loxP/loxP}$*; nestin-cre* brains was markedly increased (arrows). Scale bar represents 150 μm. SVZ, subventricular zone; VZ, ventricular zone. (**e**) Quantification of western blot data. Three independent blots per each condition were used for quantification. * $P < 0.01$.
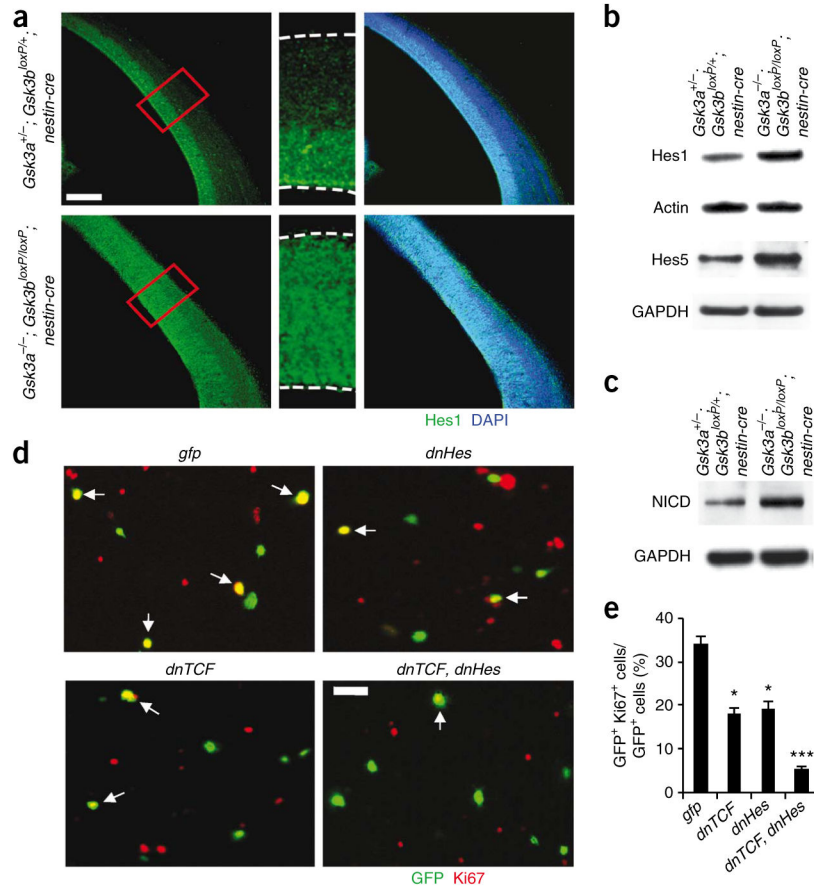
Figure 6.
Changes in Notch signaling components and contributions of β-catenin and Notch signaling to GSK-3 deletion effects. (**a**) Expanded zone of Hes1 expression in $Gsk3a^{-/-}$; $Gsk3b^{loxP/loxP}$; nestin-cre brains. Left, in control brain sections at E14, Hes1 was mostly expressed in the ventricular and subventricular zone, where progenitors are normally located. However, Hes1 was distributed throughout the developing cortical wall in $Gsk3a^{-/-}$; $Gsk3b^{loxP/loxP}$; nestin-cre cerebral cortex. Middle, higher magnification of small boxes (red) from the left panels. Right, Hes1-stained fields were merged with DAPI-stained images. Scale bar represents 150 μm. (**b**) Western blotting showed that the level of Hes1 and Hes5 were significantly increased in the $Gsk3a^{-/-}$; $Gsk3b^{loxP/loxP}$; nestin-cre brain lysates. (**c**) The level of NICD was markedly increased in $Gsk3a^{-/-}$; $Gsk3b^{loxP/loxP}$; nestin-cre brain lysates. (**d**) Inhibition of either β-catenin signaling or Notch signaling partially blocked proliferation of $Gsk3a^{-/-}$; $Gsk3b^{loxP/loxP}$; nestin-cre cortical progenitors in culture. GSK-3 mutant cells were transfected with dnTCF, dnHes or control gfp. Cells were then cultured for 48 h and immunostained with antibody to Ki67. Overexpressing both dnTCF and dnHes suppressed proliferation of GSK-3 mutant progenitors to a higher degree than overexpression of either dnTCF or dnHes alone. Scale bar represents 25 μm. Arrows indicate transfected cells that were also positive for Ki67. (**e**) The percentages of Ki67- and GFP-positive cells relative to total transfected cells (GFP positive) were counted for quantification. * $P < 0.01$ (versus GFP), ** $P < 0.01$ (versus dnTCF or dnHes).
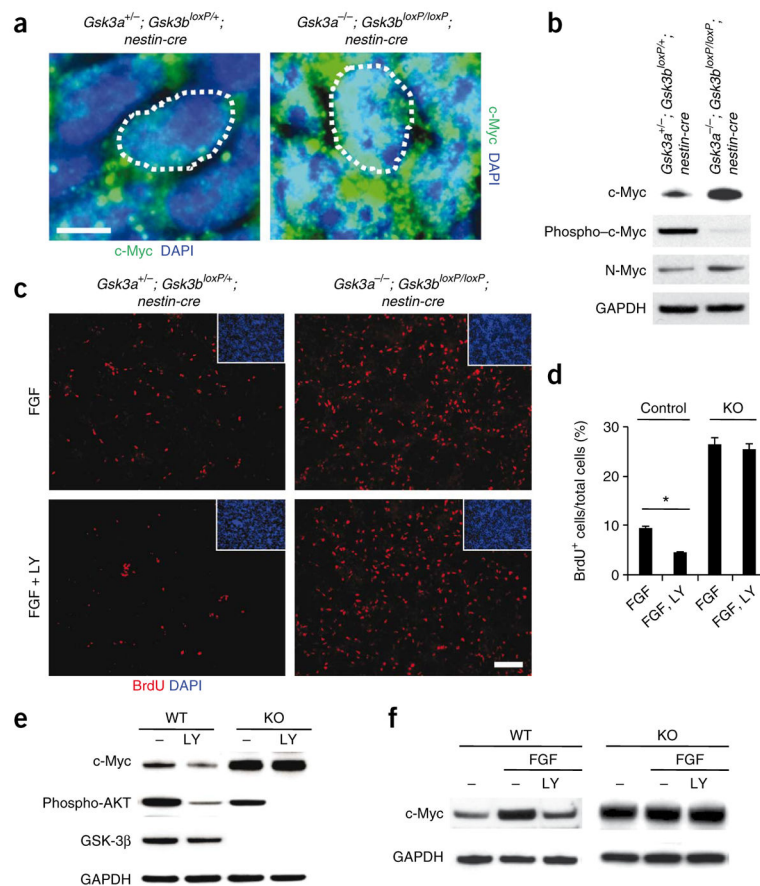
Figure 7.
GSK-3 mediates FGF-PI3K signaling to regulate c-Myc in neural progenitors. (**a**) Compared with control progenitors, c-Myc levels were massively increased in nuclei (white dotted circle) of *Gsk3a⁻/⁻; Gsk3b^{loxP/loxP}; nestin-cre* progenitors at E14. Scale bar represents 5 μm. (**b**) Western blots showed that levels of c-Myc and N-Myc were increased in GSK-3 mutant brain lysates. In contrast, phospho–c-Myc was barely detectable in GSK-3 mutant brains. (**c**) FGF effects on progenitor proliferation were mediated in part by PI3K and GSK-3. Cortical progenitors from control and GSK-3 mutant tissues were cultured with either FGF2 alone or FGF2 and LY29400 (LY) for 24 h. Then, the cultures were treated with BrdU for 6 h and immunostained with an antibody to BrdU. Treatment with FGF increased progenitor proliferation in control cultures and PI3K inhibited the FGF2 effects. GSK-3 mutant progenitors showed no response to LY29400. Scale bar represents 70 μm. (**d**) The percentage of BrdU-positive cells was counted for quantification. * $P < 0.01$. (**e**) GSK-3 mediated PI3K regulation of c-Myc. Changes in c-Myc expression with LY294002 treatment were abrogated in *Gsk3a⁻/⁻; Gsk3b^{loxP/loxP}; nestin-cre* cortical cultures. The decrease in phospho-AKT and phospho–GSK-3β showed the efficiency of PI3K inhibition. (**f**) GSK-3 mediated the effects of FGF signaling on c-Myc regulation. Western blots showed that the addition of a recombinant human basic FGF2 (10 ng ml⁻¹) in control cultures markedly induced upregulation of c-Myc, which was suppressed by LY294002 treatment. However,

neither the upregulation by FGF2 nor its suppression by LY294002 were observed in *Gsk3a*$^{-/-}$; *Gsk3b*$^{loxP/loxP}$; *nestin-cre* cortical cultures.